TISSUE ENGINEERING: Part A
Volume 21, Numbers 13 and 14, 2015

DOI: 10.1089/ten.tea.2014.0455

Salicylic Acid-Based Polymers for Guided Bone Regeneration Using Bone Morphogenetic Protein-2

Sangeeta Subramanian, BS,[1] Ashley Mitchell, MS,[1] Weiling Yu, BSEng,[2] Sabrina Snyder, PhD,[2] Kathryn Uhrich, PhD,[3] and J. Patrick O'Connor, PhD[1]

Bone morphogenetic protein-2 (BMP-2) is used clinically to promote spinal fusion, treat complex tibia fractures, and to promote bone formation in craniomaxillofacial surgery. Excessive bone formation at sites where BMP-2 has been applied is an established complication and one that could be corrected by guided tissue regeneration methods. In this study, anti-inflammatory polymers containing salicylic acid [salicylic acid-based poly(anhydride-ester), SAPAE] were electrospun with polycaprolactone (PCL) to create thin flexible matrices for use as guided bone regeneration membranes. SAPAE polymers hydrolyze to release salicylic acid, which is a nonsteroidal anti-inflammatory drug. PCL was used to enhance the mechanical integrity of the matrices. Two different SAPAE-containing membranes were produced and compared: fast-degrading (FD-SAPAE) and slow-degrading (SD-SAPAE) membranes that release salicylic acid at a faster and slower rate, respectively. Rat femur defects were treated with BMP-2 and wrapped with FD-SAPAE, SD-SAPAE, or PCL membrane or were left unwrapped. The effects of different membranes on bone formation within and outside of the femur defects were measured by histomorphometry and microcomputed tomography. Bone formation within the defect was not affected by membrane wrapping at BMP-2 doses of 12 μg or more. In contrast, the FD-SAPAE membrane significantly reduced bone formation outside the defect compared with all other treatments. The rapid release of salicylic acid from the FD-SAPAE membrane suggests that localized salicylic acid treatment during the first few days of BMP-2 treatment can limit ectopic bone formation. The data support development of SAPAE polymer membranes for guided bone regeneration applications as well as barriers to excessive bone formation.

Introduction

Bone morphogenetic protein-2 (BMP-2) is used to promote bone regeneration in spinal fusions, tibia fractures, and oral maxillofacial bone healing.[1–4] Although BMP-2 can be beneficial in regenerating bone, BMP-2 treatment can cause ectopic bone formation by inducing bone formation outside of the target volume and into surrounding tissues.[5–11] Adverse effects of BMP-2 use have been documented in patients undergoing spinal fusion, including pain, limited range of motion, difficulty swallowing, and difficulty breathing.[12–15] In some cases, corrective surgical procedures were required to treat the adverse effects of BMP-2 use. A retrospective study showed that BMP-2 use in cervical spinal fusion procedures resulted in significantly longer hospital stays and higher mortality rates.[16]

Developing methods to better regulate BMP-2 activity and limit the volume in which BMP-2 acts could increase the clinical efficacy of BMP-2 while reducing the incidence of adverse events.

Porous polytetrafluoroethylene (PTFE) and other membranes have been used as physical barriers in guided bone regeneration procedures for augmentation of the maxilla or mandible.[17,18] PTFE membrane is used as a physical barrier to soft tissue ingrowth that preserves the presumptive site of bone formation.[19] A second surgery is needed to remove the PTFE membrane once healing is complete. Biodegradable and bioresorbable membranes have been tested for guided bone regeneration efficacy in various animal models, including long bone segmental defects.[20]

Given the established efficacy of using membranes for guided bone regeneration, we considered whether a similar approach could be used to limit or restrict BMP-2 activity to a defined volume of interest. Nonsteroidal anti-inflammatory drugs (NSAIDs) can delay or prevent bone formation by inhibiting cyclooxygenase-2 (COX-2).[21–25] However, exogenous

[1]Department of Microbiology, Biochemistry and Molecular Genetics, New Jersey Medical School, Rutgers, The State University of New Jersey, Newark, New Jersey.
[2]Department of Biomedical Engineering, School of Engineering, Rutgers, The State University of New Jersey, Piscataway, New Jersey.
[3]Department of Chemistry and Chemical Biology, School of Arts and Sciences, Rutgers, The State University of New Jersey, Piscataway, New Jersey.

BMP-2 treatment can overcome the effects of NSAIDs in bone repair.[26,27] Thus, we tested a novel method to promote healing of femur segmental defects in rats by using a salicylic acid-based poly(anhydride-ester) (SAPAE) membrane as a physical barrier and localized salicylic acid (SA) delivery system to restrict BMP-2 activity to a specified region. SAPAE is a polymer that hydrolyzes to release SA (Fig. 1A), which is an NSAID that can reduce bone formation.[28] For this study, fast-degrading SAPAE (FD-SAPAE) and slow-degrading SAPAE (SD-SAPAE) polymers were used that release SA at faster and slower rates, respectively. The SAPAE polymers were mixed with polycaprolactone (PCL) to produce flexible membranes. The efficacy of FD-SAPAE and SD-SAPAE membranes at reducing BMP-2-induced ectopic bone formation, while simultaneously allowing bone formation, in rat femur defects was evaluated.

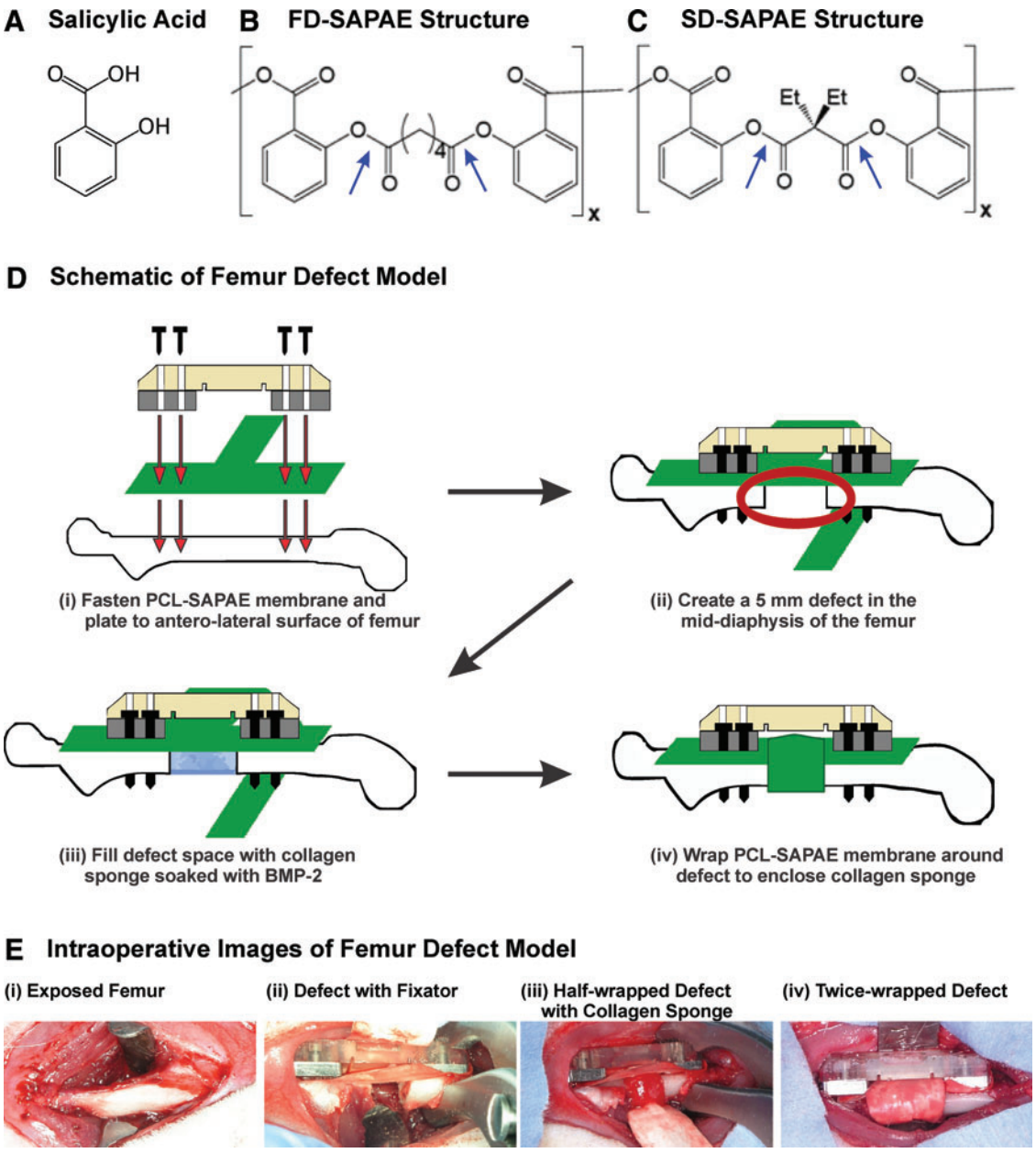

FIG. 1. Polymer structures and femur defect model. Shown are structures for **(A)** salicylic acid, **(B)** the FD-SAPAE polymer, and **(C)** the SD-SAPAE polymer. Hydrolysis sites for the FD-SAPAE and SD-SAPAE polymers are shown using *blue arrows*. **(D)** The schematic summarizes the steps (i, ii) used to create and stabilize the femur defect, (iii) treat with BMP-2 applied using a collagen sponge (*blue*), and (iv) wrap with the guided bone regeneration membrane (*green*). **(E)** Shown are intraoperative images of (i) an exposed rat femur, (ii) femur with segmental defect and fixator in place, (iii) defect filled with collagen sponge and half-wrapped with membrane, and (iv) defect with the collagen sponge (not visible) wrapped twice with the membrane and ready for wound closure. FD-SAPAE, fast-degrading SAPAE; BMP-2, bone morphogenetic protein-2; SAPAE, salicylic acid-based poly(anhydride-ester); SD-SAPAE, slow-degrading SAPAE. Color images available online at www.liebertpub.com/tea

Materials and Methods

Membrane preparation and characterization

Polymers. PCL-SAPAE membranes were synthesized according to previously described methods.[29–32] The FD-SAPAE polymer (poly[1,6-bis(o-carboxyphenoxy) hexanoate]) had an average molecular weight (Mw) of 13,400, polydispersity index (PDI) of 1.7, and a glass transition temperature (Tg) of 46°C (Fig. 1B). The SD-SAPAE polymer was synthesized using 2,2′-bis(o-carboxyphenoxy)-pentanoate and had a Mw of 26,100, PDI of 1.4, and Tg of 70°C (Fig. 1C). All chemicals and reagents, including PCL (70,000–90,000 g/mole), were purchased from Sigma-Aldrich (Milwaukee, WI) and used as received. PCL density was given by Sigma-Aldrich as 1.145 g/mL. SAPAE polymer density was measured gravimetrically.[33]

Membrane production. Electrospun membranes were produced by mixing each SAPAE with PCL in dichloromethane and dimethylformamide (1:1 volume ratio) to 25% total polymer weight (w/v). Each polymer mixture was transferred to a 10-mL syringe with a blunt 18G stainless steel needle (Popper & Sons, Inc., New Hyde Park, NY). The syringe was placed in a syringe pump set to a 5 mL/h flow rate. Positive voltage was applied to the needle tip, between 8 and 15 kV, as required to maintain steady fiber extrusion from the needle. Samples were spun onto a rotating mandrel covered with aluminum foil with a negatively charged collecting plate (5 kV) placed behind the mandrel. The mandrel was 15 cm from the needle and rotated at 60 rpm, which did not cause fiber alignment (data not shown). Membranes were cut to size and sterilized by gamma irradiation (18 gray) for *in vivo* testing.

Membrane morphology. Membrane samples were sputter coated with Au/Pd (SCD 004 Sputter Coater; Bal-Tec, Balzers, Liechtenstein) and observed by scanning electron microscopy (AMRAY 1830I; AMRAY, Inc., Bedford, MA). Average fiber diameter was determined using ImageJ, and images were taken from 4 areas of each sample with 25 fiber measurements per image.[34] Membrane porosity was determined as described previously.[33]

Mechanical testing. The electrospun PCL, FD-SAPAE, and SD-SAPAE membranes were cut into dog-bone shapes with an approximate 5 mm minimum width and subjected to uniaxial tensile loading at room temperature (EnduraTEC ELF 3200 Dynamic Mechanical Analyzer; Bose Corp., Framingham, MA). Data were collected using WinTest software (Version 4.1; Bose Corp.). The minimum sample width and thickness were recorded before testing. Strain was ramped at 0.05 mm/s with an initial displacement of 5 mm between clamps and increased until membrane failure. Membranes were tested dry and after soaking in phosphate-buffered saline (PBS) for 30 min. Stress was calculated using a Poisson coefficient of 0.45.[33] Elastic moduli were determined from the slopes of best-fit lines for the initial linear portion of the graphs.

Salicylic acid release. Four pieces of each membrane (5 × 5 mm) were weighed and then immersed in 1 mL of PBS with gentle shaking at 37°C. The PBS was collected and replaced with 1 mL of fresh PBS at time points ranging from 1 h to 28 days. SA in each PBS sample was measured by absorbance following separation on an Eclipse XDB-C18 column (4.6 × 150 mm) using a Dionex DX-500 system (Sunnyvale, CA). The SA in 25 μL of each PBS sample was separated isocratically using 75% PBS and 25% acetonitrile at a flow rate of 0.3 mL/min. SA eluted at 5.2–5.4 min, and the area under the A_{303nm} curve for each sample peak was determined using Chromeleon 6.7 software. Data were compared to SA standards to determine the amount of SA in each sample.

Water retention and swelling. Pieces of each membrane type (5 × 5 mm) were weighed and then submerged in PBS for 28 days. The membrane pieces were removed, blotted dry, and weighed after 1, 2, 4, 8, and 24 h and at 2, 4, 8, 9, 10, 14, 21, and 28 days.

Protein diffusion. A Franz cell (PermeGear, Hellertown, PA) was used to measure protein diffusion across each membrane. Air trapped in the membranes was removed by soaking the membranes for 5 min in PBS under vacuum and then sonicating the vacuum flask containing the membranes for 1 min. Each membrane was then placed in the Franz cell to measure diffusion of bovine serum albumin (BSA, 10 mg/mL in PBS, Mw of 66.5 kDa) across the membrane into PBS. Samples of 100 μL were collected from the Franz cell at 0, 1, 2, 4, and 8 h, and BSA concentration was measured using the bicinchoninic acid (BCA) method.[35] For FD-SAPAE, the membrane also was tested 4 h after being wetted under vacuum, followed by 1 min of sonication.

Femur defect model

Surgical procedure. Male Sprague-Dawley rats weighing ~450 g were used (Taconic Farms, Inc., Germantown, NY). Femur segmental defects were made as described previously.[36] Rats were treated preoperatively with enrofloxacin (22.7 mg/kg, intramuscular injection) and buprenorphine (0.05 mg/kg, subcutaneous injection). The rats were anesthetized with ketamine (60 mg/kg) and xylazine (10 mg/kg) by intraperitoneal injection. The right hind limb was shaved, scrubbed with povidone–iodine, and draped.

A 4-cm incision was made on the lateral surface of the thigh, followed by blunt dissection of the musculature to expose the femur. The periosteum on the mid-diaphysis of the femur was scraped away. A custom fixator comprising two small stainless steel plates connected with a high-density polyethylene plate was applied to the femur to stabilize the femur and anchor the membrane to the bone.[36] A 5-mm defect was created using a sagittal saw. The defect space was irrigated with saline, and then filled with a collagen sponge soaked in a recombinant human BMP-2 solution. The membrane was wrapped around the femur twice to enclose the defect space (Fig. 1D, E). No membrane was used in the control group. The wound was closed in layers using resorbable sutures, and topical antibiotic cream was applied to the incision site.

Rats were treated with enrofloxacin for 2 days after surgery to prevent infection. Weekly radiographs were taken to ensure proper fixation and to monitor healing. All animals

were euthanized 4 weeks postsurgery. All animal procedures were approved by the Rutgers New Jersey Medical School Institutional Animal Care and Use Committee.

Bone morphogenetic protein-2 dosage and delivery. Clinically, BMP-2 is delivered using collagen sponge as the carrier.[4,37,38] Previous experiments have shown that collagen sponge provides for controlled logarithmic release of BMP-2 in rats for at least 1 week.[39] For this study, recombinant human BMP-2 (Medtronic, Inc., Minneapolis, MN) was diluted with BMP-2 buffer (5 mM glutamate, 5 mM sodium chloride, 2.5% glycine, and 0.5% sucrose, pH 4.5) to final concentrations of 35, 120, or 240 μg/mL.[40,41] One hundred microliters of diluted BMP-2 was evenly pipetted onto $15 \times 15 \times 2.75$ mm Helistat absorbable collagen sponges (Integra Life Sciences, Plainsboro, NJ) to deliver 3.5, 12, or 24 μg of BMP-2. All of the BMP-2 solution was absorbed by the collagen sponge. Controls used a collagen sponge treated only with BMP-2 buffer. The saturated collagen sponge was inserted into the femoral defect, and then wrapped with a membrane as described above.

Outcome measurements

Microcomputed tomography. Three-dimensional microcomputed tomography (microCT) images were used to measure bone volume (BV; mm^3) within and outside (ectopic) the defect site. The right femur was excised, fixed in 10% formalin, and transferred into 70% ethanol before scanning. Samples were scanned using a Bruker Skyscan 1172 scanner (Micro Photonics, Inc., Allentown, PA) at 70 kVp, 142 mA, and 12 μm voxel size with a 0.5-mm aluminum filter to reduce beam hardening. Images were reconstructed with NRecon and analyzed with CTAn software provided by the manufacturer. Two different volumes of interest were analyzed; (i) the defect bone volume defined by the proximal and distal edges of the defect and extending laterally to the peripheral margin of the original femur and (ii) the ectopic bone volume defined as total new bone volume minus defect bone volume. microCT analysis was not done for the BMP-2 dose–response experiment.

Histology and histomorphometry. Following microCT, samples were dehydrated through grades of ethanol, cleared in xylene, and embedded in poly(methyl methacrylate). Sagittal sections were cut, polished, and stained with Stevenel's blue and Van Gieson's picrofuchsin for soft and mineralized tissue, respectively.[42] Digital images were captured using an Olympus SZ-40 microscope (Olympus Corporation of America, Center Valley, PA) and a SPOT Idea camera (Diagnostic Instruments, Inc., Sterling Heights, MI). New bone area (BA; mm^2) and new bone area per total area (BA/TA; %) were measured in the defect and ectopic bone regions for each sample using ImagePro Premier 9.0 Software (Media Cybernetics, Inc., Rockville, MD). The defect bone area was defined by the proximal and distal edges of the defect and extended laterally to the peripheral margins of the original femur. The ectopic bone area was defined as total new bone area minus defect bone area.

Statistical analyses. The BMP-2 dose–response data were analyzed using a three-way ANOVA and *post hoc* Fisher's tests to isolate effects between groups. BMP-2 dose, membrane use, and bone formation location (defect and ectopic) were the independent variables, while bone area was the dependent variable. For membrane comparisons, microCT and histological data were compared separately using two-way ANOVA and *post hoc* Fisher's tests to isolate effects between groups. Membrane type and bone formation location were the independent variables, while bone area for the histomorphometry data and bone volume for the microCT data were the dependent variables. Statistical calculations were performed using SigmaPlot version 12.5 software (Systat Software, Inc., San Jose, CA).

Results

Membrane characteristics

SAPAE-PCL electrospun membranes were produced using 0, 20, 40, 60, 80, or 100 weight percent SAPAE. Membranes were tested for fiber diameter, porosity, and tensile testing to determine elasticity (data not shown). The elastic modulus of the FD-SAPAE (250 kPa) and SD-SAPAE (425 kPa) membranes peaked at 40% SAPAE and 60% PCL. Prewetting the membranes had no significant effect on the elastic modulus. Consequently, the 40% SAPAE and 60% PCL membranes were used in the subsequent studies. Fiber diameter was 0.60 ± 0.27 and 0.96 ± 0.42 μm for the FD-SAPAE and SD-SAPAE membranes, respectively. Percent porosity $[(1 - (\text{membrane density/material density})) \times 100\%]$ was $69.13\% \pm 0.08\%$ and $74.59\% \pm 0.08\%$ for the FD-SAPAE and SD-SAPAE membranes, respectively.

The ability of the FD-SAPAE, SD-SAPAE, and PCL membranes to retain water was evaluated over a period of 28 days (Fig. 2A, B). The PCL membranes did not retain water. The FD-SAPAE membrane rapidly gained water weight between 2 and 8 h (Fig. 2A), and then slowly started to lose weight between 8 h and 28 days (Fig. 2B). The SD-SAPAE membranes experienced nearly no change in weight until day 2, after which the SD-SAPAE membranes steadily gained water weight (Fig. 2B).

SA release from each membrane (25 mm^2) was measured at 1, 2, 4, 8, and 24 h (Fig. 2C), and then daily for 28 days (Fig. 2D). On average, 51 μg of SA was released from each FD-SAPAE membrane between 0 and 3 days, while an additional 9 μg of SA was released from each FD-SAPAE membrane between days 4 and 28. In contrast, most of the SA released from the SD-SAPAE membranes occurred after day 9. Less than 1 μg of SA was released from each SD-SAPAE between 0 and 9 days, while 9.5 μg of SA was released from each SD-SAPAE membrane between days 10 and 28.

Membrane permeability was assessed by measuring diffusion of BSA across each membrane. BSA concentrations reached equilibrium in less than 24 h when each membrane type was tested as a diffusion barrier (data not shown). The rapid gain in water weight for the FD-SAPAE membrane suggests that membrane fibers swell with water, which could affect diffusion of BSA across the membrane. However, when the FD-SAPAE membrane was prewetted for 4 h before assessing BSA diffusion across the membrane, no increase in time required to reach equilibrium was detected. Because the active form of BMP-2 has a Mw (26 kDa) less

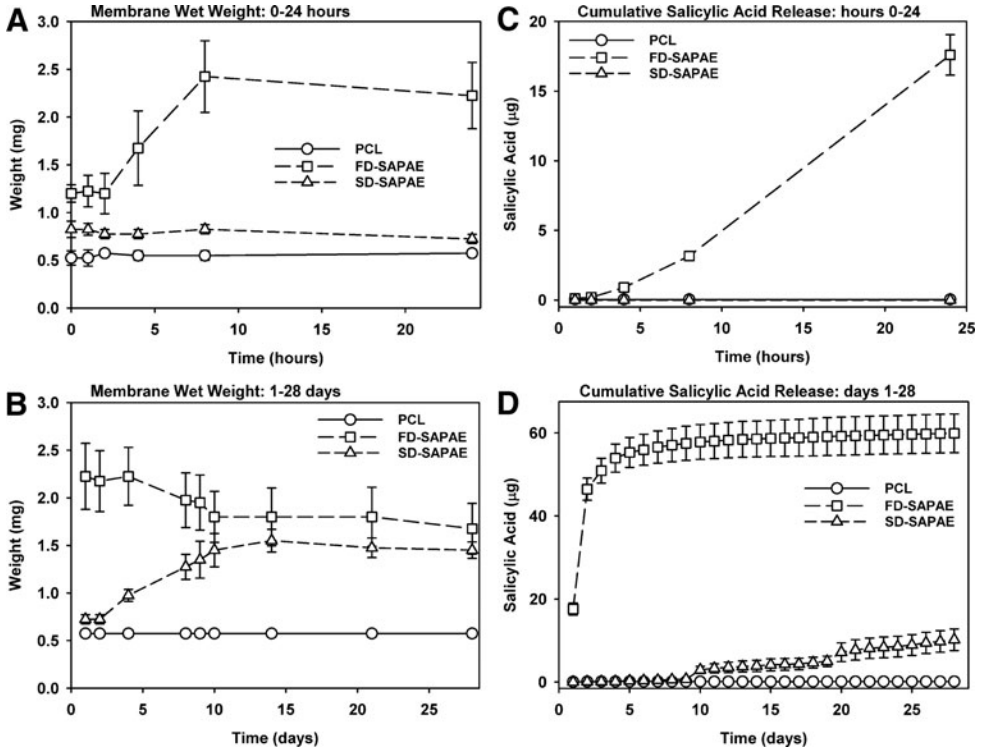

FIG. 2. SAPAE membrane hydrolysis. FD-SAPAE, SD-SAPAE, and PCL membranes were cut into 5×5 mm squares and weighed ($n=4$). The membrane pieces were then incubated in PBS at 37°C for 28 days to measure the increase in membrane weight **(A, B)** or salicylic acid release **(C, D)**. To measure membrane wet weight, each membrane piece was removed from the PBS at the indicated times, blotted dry, weighed, and then returned to the PBS. Shown are mean weights (±SE) for the PCL (*circles*), FD-SAPAE (*squares*), and SD-SAPAE (*triangles*) membrane pieces between 0 and 24 h **(A)** and 1 and 28 days **(B)**. To measure salicylic acid release, the PBS was collected and replaced at the times indicated. The amount of salicylic acid in each sample was determined by HPLC and UV absorbance. Shown are the mean cumulative amounts of salicylic acid released (±SE) for membrane pieces between 1 and 24 h **(C)** and 1 and 28 days **(D)**. PBS, phosphate-buffered saline; PCL, polycaprolactone.

than BSA (66.5 kDa), the membranes are not expected to inhibit BMP-2 diffusion.

Disposition of the animals

The different experimental groups, the number of rats used in each, and sample disposition are summarized in Table 1. Fifty-five animals underwent surgery for this study. Four rats were euthanized because of fixation failure and were excluded from the study. Four histological samples were not used due to poor specimen processing. Only samples from the 12-μg BMP-2 dose groups were used for microCT analysis. No infections or other postsurgery complications were noted in any of the animals used for analysis.

Table 1. Summary of Group Sizes

BMP-2 dose (μg)	*Membrane*	*X-rays*	*Histomorphometry*	*microCT*
0	—	3	3	—
3.5	—	3	3	—
12	—	6	6	6
24	—	3	3	—
0	FD-SAPAE	3	2	—
3.5	FD-SAPAE	3	3	—
12	FD-SAPAE	9	8	9
24	FD-SAPAE	3	2	—
12	PCL	9	8	9
12	SD-SAPAE	9	9	9

BMP-2, bone morphogenetic protein-2; FD-SAPAE, fast-degrading SAPAE; microCT, microcomputed tomography; PCL, polycaprolactone; SAPAE, salicylic acid-based poly(anhydride-ester); SD-SAPAE, slow-degrading SAPAE.

FD-SAPAE membrane inhibits BMP-2-induced ectopic bone formation

A dose–response analysis was used to determine whether BMP-2-induced ectopic bone formation was dose-dependent in the rat femur defect model and whether the FD-SAPAE membrane would inhibit bone formation. Radiographs and histological sections of femurs treated with 0, 3.5, 12, or 24 μg of BMP-2 and without any membrane wrapping indicated that maximal bone formation in and outside the defect volume occurred with 12 μg of BMP-2 (Fig. 3). Conversely, radiographs and histology indicated that the FD-SAPAE membrane did not inhibit bone formation within the femur defect at BMP-2 doses greater than 3.5 μg, but did reduce ectopic bone formation.

Histomorphometry was used to quantify the amount of bone formed within the defect region and ectopic bone formed outside the defect region (Fig. 4). The 12-μg BMP-2 dose produced the most new bone with 15.8 mm^2 formed in the no membrane group and 11.9 mm^2 formed in the FD-SAPAE

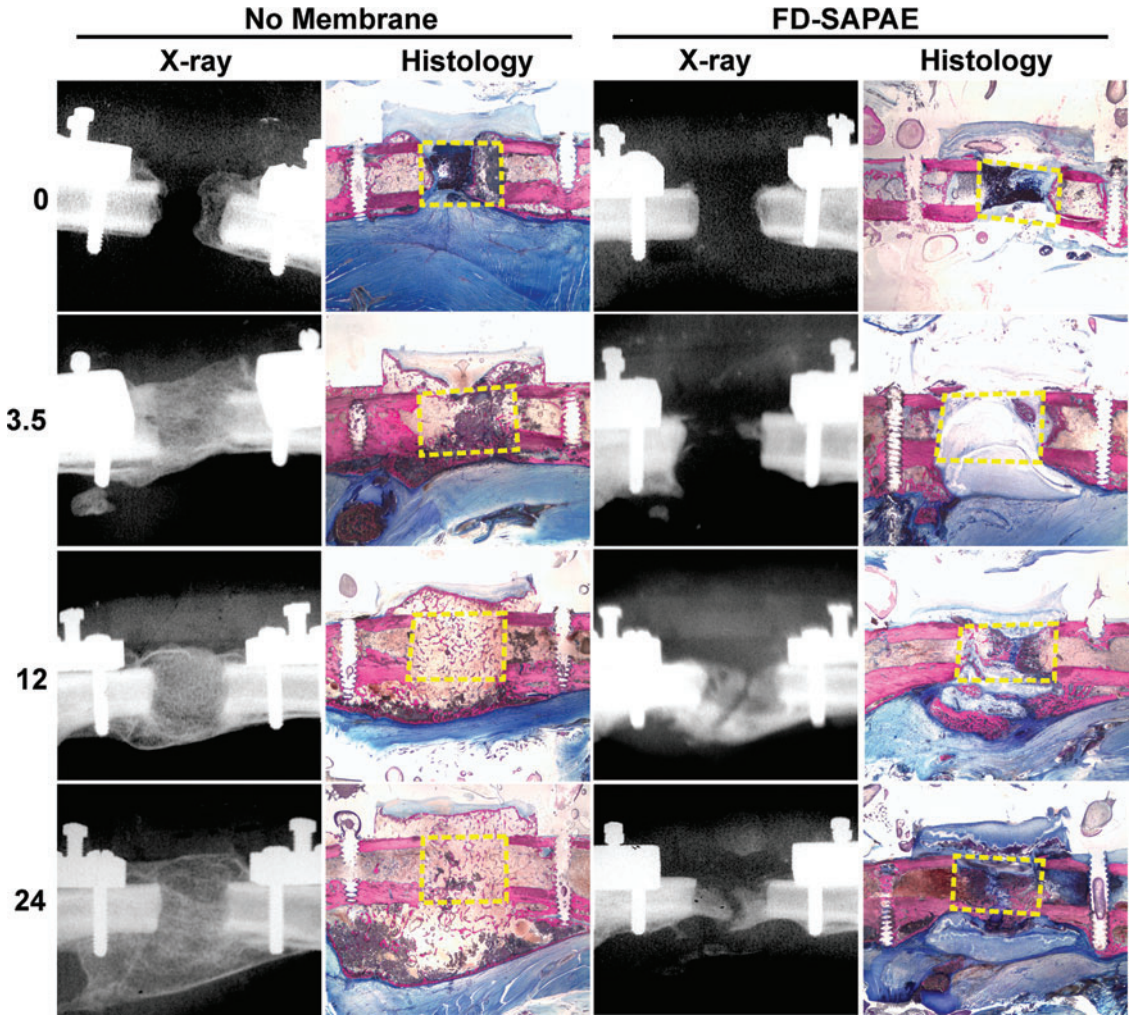

FIG. 3. Bone morphogenetic protein-2-induced bone formation occurs within the defect of FD-SAPAE membrane-wrapped femurs. The dose–response effects of BMP-2 on bone formation within and outside rat femur defects were assessed by radiographic (X-ray) and histological (histology) observations 4 weeks after surgery. BMP-2 doses used were 0, 3.5, 12, and 24 μg applied to a collagen sponge inserted in the segmental defect. The defect was left unwrapped (no membrane) or wrapped with the FD-SAPAE membrane (FD-SAPAE). Defect areas in the histology images are indicated using the hatched *yellow lines*. Color images available online at www.liebertpub.com/tea

membrane group. Most of the bone that formed in the 12-μg no membrane group was ectopic with almost four times more ectopic (12.6 mm^2) than defect area new bone (3.2 mm^2). In contrast, only 1.4 times more ectopic bone (6.9 mm^2) than defect area new bone (5.0 mm^2) was formed in the 12-μg FD-SAPAE membrane group. The histomorphometry data were compared using three-way ANOVA and *post hoc* Fisher's tests (Table 2). Bone formation was BMP-2 dose dependent ($p = 0.001$) and independent of location (defect vs. ectopic) or membrane use. Maximum bone formation occurred at a minimum BMP-2 dose of 12 μg ($p = 0.003$ vs. 3.5 μg), which was consistent with previous findings.[41] In contrast, a significant interaction was observed between use of the FD-SAPAE membrane and the location of new bone formation. The FD-SAPAE membrane significantly reduced ectopic bone formation ($p < 0.001$). The amount of ectopic bone was significantly greater than defect bone in the unwrapped femurs ($p < 0.001$), whereas no difference was detected in the FD-SAPAE membrane-wrapped femurs ($p = 0.984$).

Reduced ectopic bone formation with localized SA delivery

The reduced ectopic bone formation observed in the femurs wrapped with the FD-SAPAE membrane could be caused by the FD-SAPAE membrane acting as a physical barrier or by SA released from the membrane causing local inhibition of bone formation.[28] To distinguish between these possible mechanisms, additional membranes were tested using the rat femur defect model treated with 12 μg of BMP-2. Four groups were tested; (a) unwrapped femur defects as a control, femur defects wrapped with (b) the FD-SAPAE membrane, (c) the PCL membrane to act only as a physical barrier, or (d) the SD-SAPAE membrane that should release less SA at the defect site.

Similar to the BMP-2 dose–response analysis, radiographs and histological sections indicated that a large amount of bone formed in the unwrapped femur defects and that the FD-SAPAE membrane reduced ectopic bone formation without affecting bone formation in the defect space (Fig. 5).

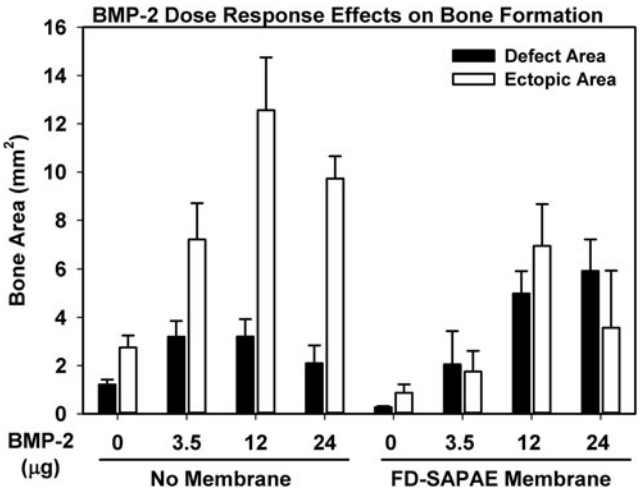

FIG. 4. The FD-SAPAE membrane reduces new bone area outside the femur defect. Rat femur defects were treated with increasing BMP-2 doses (0, 3.5, 12, and 24 μg) applied on a collagen sponge that was inserted into the femur defect. The defect was then left unwrapped (no membrane) or wrapped with the FD-SAPAE membrane. Four weeks after surgery, mean new bone area (±SE) within (defect area, *black bars*) and outside (ectopic area, *white bars*) the defects was calculated. Data were compared by ANOVA (Table 2). The 12-μg BMP-2 dose produced the most new bone. Wrapping the defect with the FD-SAPAE membrane significantly reduced bone formation outside the defect area (ectopic area; $p < 0.001$) without significantly reducing new bone area within the defect.

Wrapping the defect site with a PCL membrane appeared to enhance defect space bone formation, similar to the FD-SAPAE membrane. However, the PCL membrane did not prevent ectopic bone formation to the same extent as the FD-SAPAE membrane.

The SD-SAPAE membrane appeared to have little effect on bone formation. Ectopic bone formation in the SD-SAPAE membrane-wrapped femurs appeared to extend further into the surrounding soft tissue than any other treatment group, although the amount of ectopic bone formed was similar to the no membrane and PCL membrane groups. Gross dissection found that the SD-SAPAE membranes were associated with aseptic fluid-filled voids contiguous with the femur defect region and which had bone forming on the peripheral margins (data not shown).

Defect and ectopic bone formation were measured by microCT and histomorphometric analyses (Fig. 6). The data were analyzed by two-way ANOVA using membrane type and bone formation location (defect or ectopic) as the independent variables and bone area (histomorphometry) or bone volume (microCT) as the dependent variable (Table 3). No significant difference in defect bone area (4.4 mm^2, mean for all groups) or defect bone volume (8.1 mm^3, mean for all groups) was detected. However, the analyses found significant interactions between membrane type and bone formation location. *Post hoc* tests found significantly more ectopic bone than defect bone for each group ($p \leq 0.008$), except the FD-SAPAE membrane group ($p = 0.248$ histomorphometry, $p = 0.577$ microCT). Similarly, ectopic bone area (6.9 mm^2 vs. 11.1–12.6 mm^2) or volume (5.2 mm^3 vs. 16.5–26.7 mm^3) was significantly less in the FD-SAPAE membrane group compared with all other groups ($p \leq 0.012$). Ectopic bone volume was also less in the PCL membrane group compared with the no membrane group (16.5 mm^3 vs. 26.7 mm^3, $p = 0.005$).

Discussion

The study assessed whether a composite membrane made from slow- or fast-degrading SAPAE and PCL polymers could serve as a guided bone regeneration membrane to prevent ectopic bone growth at sites of BMP-2-induced bone formation. Initial experiments confirmed previous studies that 12 μg of BMP-2 produces a maximal bone formation response in the rat femur defect model.[41] Of the total bone formed, 71% was located outside the femur defect in the 12-μg BMP-2 dose group. Wrapping the defect with the FD-SAPAE membrane reduced the amount of bone formed outside the defect to 43% of the total new bone formed in the 12-μg BMP-2 dose group.

Table 2. Three-Way ANOVA of Membrane and BMP-2 Dose Effects on Bone Formation

		Membrane dependence	*Within no membrane group*	*Within FD-SAPAE group*
Bone area location (defect vs. ectopic)		$p = 0.003$	$p < 0.001$	$p = 0.984$
		Location dependence	*Within defect area*	*Within ectopic area*
Membrane effect on bone area (none vs. FD-SAPAE)		$p = 0.035$	$p = 0.490$	$p < 0.001$
		Membrane dependence	*Location dependence*	*Dose dependence*
BMP-2 effect on bone area		$p = 0.855$	$p = 0.145$	$p < 0.001$
	0 μg	3.5 μg	12 μg	24 μg
Comparisons between BMP-2 doses (Fishers LSD)	vs.	$p = 0.102$ vs.	$p < 0.001$ $p = 0.003$ vs.	$p = 0.007$ $p = 0.196$ $p = 0.183$

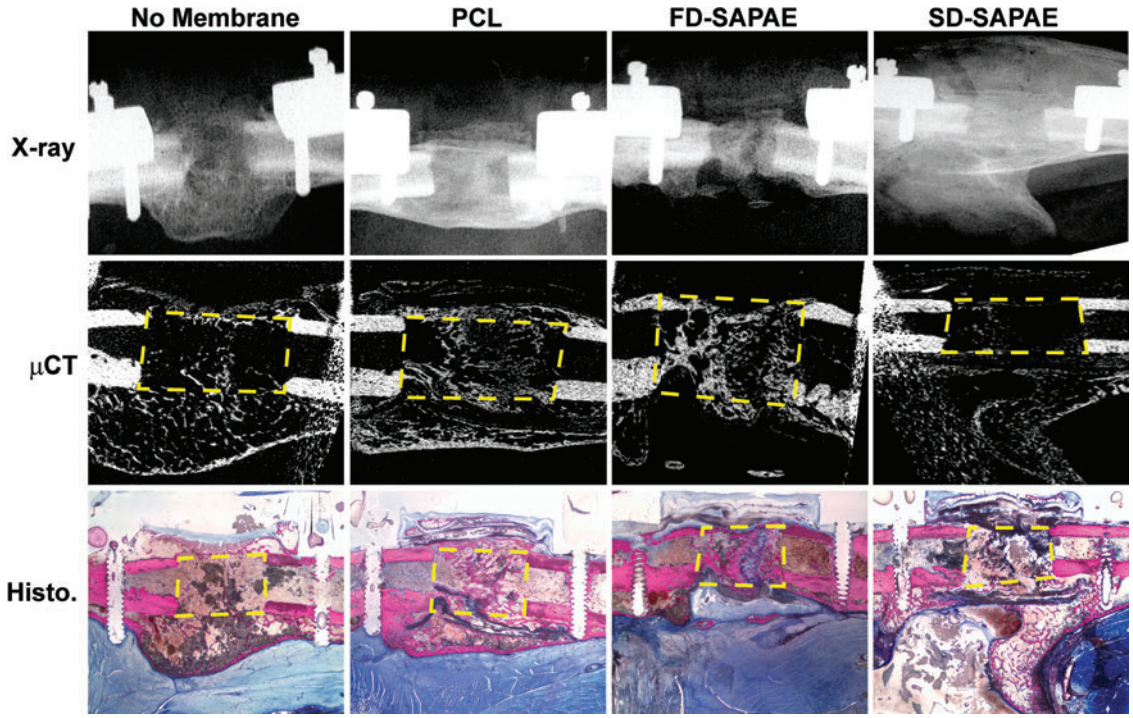

FIG. 5. Effects of membrane type on BMP-2-induced bone formation in rat femur defects. Four weeks after surgery, the effects of not wrapping (no membrane) and wrapping femur defects with electrospun PCL, FD-SAPAE, or SD-SAPAE membranes were qualitatively assessed by radiographic (X-ray), microCT, and histology (Histo.). All defects were treated with 12 μg of BMP-2 absorbed on a collagen sponge. The PCL and FD-SAPAE membranes appeared to focus bone formation within the defect, but only the FD-SAPAE membrane reduced bone formation outside the defect area. Defect regions in the microCT and histology images are indicated using hatched *yellow lines*. microCT, microcomputed tomography. Color images available online at www.liebertpub.com/tea

The amount of bone formed in the defect volume of the FD-SAPAE membrane-wrapped femurs ($6.9 \pm 2.2\,mm^3$; mean ± SE) was not statistically different from the unwrapped femurs ($11.2 \pm 2.7\,mm^3$; $\beta = 0.133$). These data show that the FD-SAPAE membrane can be used for guided bone regeneration.

The FD-SAPAE membrane appears to limit ectopic bone formation by releasing SA at the defect site. *In vitro* diffusion studies found that BSA rapidly diffused across the membranes (data not shown). Diffusion of BMP-2 across the SAPAE membranes was not directly tested. However, it is

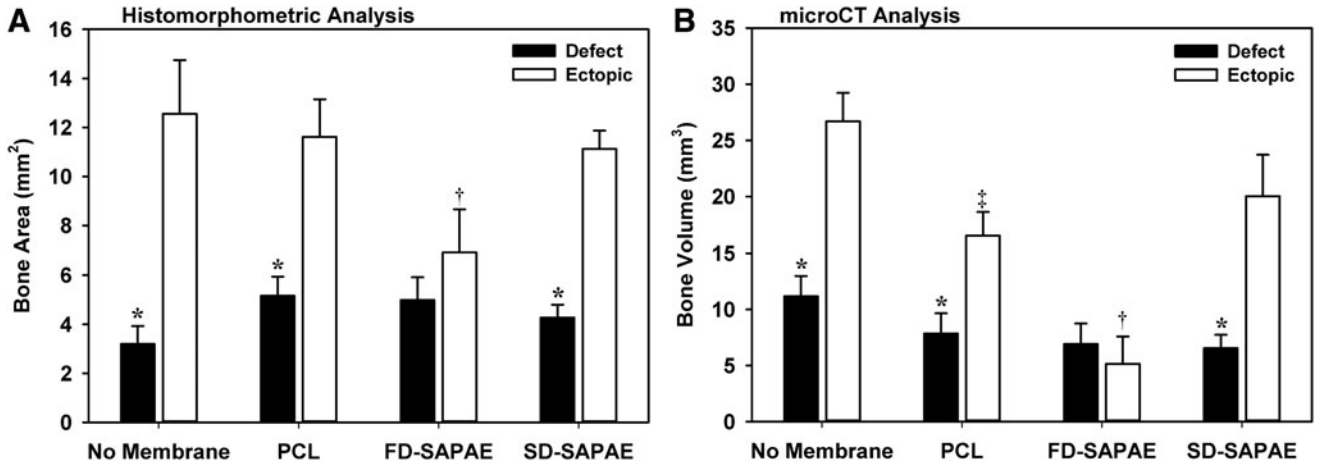

FIG. 6. Comparison of membrane effects on bone formation within and outside the femur defect. Rat segmental defects were treated with 12 μg of BMP-2 on a collagen sponge and then left unwrapped (no membrane) or wrapped with electrospun PCL, FD-SAPAE, or SD-SAPAE membranes. Four weeks after surgery, bone formation was measured by histomorphometry **(A)** and microCT **(B)**. Mean bone area or volume (±SE) within the defect (*black bars*) and outside the defect (ectopic, *white bars*) is shown. The data were compared by ANOVA (Table 3). Significant effects are noted as (*) defect bone area or volume significantly less than ectopic bone area or volume, (†) ectopic bone area or volume significantly less than all other groups, and (‡) ectopic bone volume less than no membrane wrap.

Table 3. Two-Way ANOVA for Different Membrane Effects on Bone Formation

	p-*Values from Fisher's LSD tests*			
	No membrane	*PCL*	*SD-SAPAE*	*FD-SAPAE*
Two-way ANOVA of histomorphometric data: interaction between location and membrane type, $p = 0.034$				
Ectopic vs. defect bone area	< 0.001	< 0.001	< 0.001	0.248
Defect bone area				
No membrane vs.	—	0.280	0.542	0.325
PCL vs.		—	0.587	0.917
SD-SAPAE vs.			—	0.662
Ectopic bone area				
No membrane vs.	—	0.603	0.419	0.003
PCL vs.		—	0.765	0.007
SD-SAPAE vs.			—	0.012
Two-way ANOVA of microCT data: interaction between location and membrane type, $p = 0.002$				
Ectopic vs. defect bone volume	< 0.001	0.008	< 0.001	0.577
Defect bone volume				
No membrane vs.	—	0.349	0.195	0.233
PCL vs.		—	0.683	0.771
SD-SAPAE vs.			—	0.907
Ectopic bone volume				
No membrane vs.	—	0.005	0.063	< 0.001
PCL vs.		—	0.270	< 0.001
SD-SAPAE vs.			—	< 0.001

unlikely that an interaction between BMP-2 and the FD-SAPAE membrane prevented BMP-2 from diffusing across the membrane and thereby limited ectopic bone formation since the FD-SAPAE and SD-SAPAE polymers have very similar chemical structures (Fig. 1), and no significant reduction in ectopic bone formation was observed using the SD-SAPAE membrane. Thus, it is unlikely that the FD-SAPAE membrane acts solely as a physical barrier to BMP-2 diffusion into the ectopic space.

The PCL membrane did limit ectopic bone formation compared with the no membrane control, suggesting that a physical barrier can be effective at reducing ectopic bone formation. However, the FD-SAPAE membrane significantly reduced ectopic bone formation better than the PCL or SD-SAPAE membranes.

Since SA release from the SD-SAPAE membrane is delayed, the data suggest that the timing as well as dose of SA is critical for reducing ectopic bone formation. By extrapolating the amount of SA released from the FD-SAPAE membrane *in vitro* (25 mm^2) to the size of the membrane used to wrap the femur defects ($\sim 615\ mm^2$), we estimate that 433, 710, 110, 74, and 34 μg of SA were released at the defect site during the first, second, third, fourth, and fifth days after surgery, respectively. Conversely, minimal SA was released from the SD-SAPAE until 10 days after surgery. The estimated average daily release of SA over 28 days from the FD-SAPAE and SD-SAPAE membranes used to wrap the femur defects was 53 and 9 μg, respectively. To place these values in context, the therapeutic plasma concentration for orally administered SA is 150–300 μg/mL.[43] While SA release during the first few days after surgery was effective at reducing ectopic bone formation, different SA doses during this period or an alternative dosing duration may more effectively limit ectopic bone formation without affecting bone formation within the defect.

The utility of SA for guided bone regeneration will likely reflect the amount, onset, and duration of SA dosing, as well as use of BMP-2 to induce osteogenesis. SA is a relatively poor cyclooxygenase inhibitor. In interleukin-1 beta (IL-1β)-stimulated A549 cells treated with 30 μM arachidonic acid, greater than 100 μg/mL of SA is required to inhibit 50% of COX-2 activity compared with 0.27 μg/mL of indomethacin.[44] However, SA is an NSAID, which can inhibit bone formation in high concentrations.[28,45] In this experiment, bone formation in the defect induced by 12 μg of BMP-2 was not inhibited by SA released from the SAPAE membranes. A previous study also found that BMP-2 could overcome the inhibitory effects of ketorolac on osteogenesis during spinal fusion in rabbits.[26]

The mechanism by which BMP-2 treatment overcomes the inhibitory effects of NSAIDs on osteogenesis is not known. BMP-2 can induce COX-2 expression, and COX-2 activity can induce BMP-2 expression.[46–48] These observations suggest that NSAIDs can suppress endogenous BMP-2 expression to inhibit osteogenesis and that exogenous BMP-2 treatment circumvents this inhibition. However, exogenous BMP-2-induced ectopic bone formation is reduced approximately fivefold in COX-2 null mice, suggesting that COX-2 has additional osteogenic functions than just promoting BMP-2 expression.[46] A balance between NSAID inhibition of cyclooxygenase activity and exogenous BMP-2 treatment may be necessary to produce an optimal bone formation response for directed tissue regeneration.

The mechanism by which SA released from the FD-SAPAE membrane limits ectopic bone formation is likely to be complex. SA can be an effective anti-inflammatory agent.[43] Indeed, we recently demonstrated that solvent-cast FD-SAPAE polymer inhibited local inflammation at a parietal bone defect in rabbits.[49] However, the anti-inflammatory effects of SA can occur independent of cyclooxygenase inhibition. SA has been shown to affect transcription factors (NF-κB, AP-1, cMyc, STAT1), IKK kinase, MAP kinases (Erk1/2, p38, JNK, and p90RSK), cell cycle regulatory proteins, heat shock factors, and lipoxygenase-dependent lipid peroxidation that could potentially affect bone regeneration.[43,50–52] SA can inhibit oxidative phosphorylation, leading to reduced intracellular ATP levels and secretion of adenosine, which can activate anti-inflammatory purinergic pathways.[53] In a mouse air pouch model of carrageenan-induced inflammation, therapeutic millimolar concentrations of SA inhibited inflammation in mice lacking COX-2 or NF-κB activity, but the SA anti-inflammatory activity was lost when wild-type mice were also treated with adenosine deaminase or the adenosine A_2 receptor antagonist, 3,7-dimethyl-1-propargylxanthine.[54] We suggest that in the present model, locally high concentrations of BMP-2 in the femur defect can overcome any SA-induced inhibition of osteogenesis, but SA released into the ectopic space alters the inflammatory response, which limits the amount or types of cells necessary for bone formation.[55,56]

A significant advantage of using an SAPAE membrane for guided bone regeneration is that membrane characteristics, including SA release and membrane physical characteristics, can be altered to optimize effectiveness. SA release rate and

polymer pliability varies between different SAPAE polymers.[57–59] SAPAE polymers comprise SA joined by a linker molecule. The kinetics of SA hydrolysis from SAPAE polymers can be altered by changing the linker molecule as shown previously and as shown here with the FD-SAPAE and SD-SAPAE polymers (Figs. 1 and 4).[59]

Normally, SAPAE polymers are brittle. A previous study showed that SAPAE polymer pliability and SA release can be changed by copolymerization of different SAPAE monomers.[60] In this study, PCL was electrospun with the FD-SAPAE or the SD-SAPAE polymer to improve the handling characteristics of the electrospun membrane. Composite membranes containing 60% PCL and 40% SAPAE were found to have optimal handling characteristics, which included sufficient pliability to wrap the femur defect. *In vivo*, the histological processing of the resected femurs would have dissolved any remaining polymer and therefore the status of the membrane was not determined. *In vitro*, however, the SAPAE-PCL membranes were physically intact after 28 days in PBS (not shown) even though significant amounts of SA had been hydrolyzed (Fig. 2). These data suggest that the PCL polymer was still intact, which would be consistent with established *in vitro* and *in vivo* degradation rates for PCL.[61,62]

The experiments clearly show that the FD-SAPAE membrane reduced ectopic bone formation more than the SD-SAPAE or PCL membranes. Additional experiments are needed to understand the temporal and dose–response relationships between SA release and BMP-2-induced bone formation and SA effects on osteoinductive or osteoconductive bone formation.

Acknowledgment

This project was supported by Award Number R01DE019926 from the National Institute of Dental and Craniofacial Research. The content is solely the responsibility of the authors and does not necessarily represent the official views of the National Institute of Dental and Craniofacial Research or the National Institutes of Health.

Disclosure Statement

No competing financial interests exist.

References

1. Kraiwattanapong, C., Boden, S.D., Louis-Ugbo, J., Attallah, E., Barnes, B., and Hutton, W.C. Comparison of Healos/bone marrow to INFUSE(rhBMP-2/ACS) with a collagen-ceramic sponge bulking agent as graft substitutes for lumbar spine fusion. Spine **30,** 1001, 2005.
2. Glassman, S.D., Carreon, L., Djurasovic, M., Campbell, M.J., Puno, R.M., Johnson, J.R., and Dimar, J.R. Posterolateral lumbar spine fusion with INFUSE bone graft. Spine J **7,** 44, 2007.
3. Arzi, B., Verstraete, F.J., Huey, D.J., Cissell, D.D., and Athanasiou, K.A. Regenerating mandibular bone using rhBMP-2: part 1-immediate reconstruction of segmental mandibulectomies. Vet Surg 2014. [Epub ahead of print]; DOI: 10.1111/j.1532-950x.2014.12123.x.
4. Govender, S., Csimma, C., Genant, H.K., Valentin-Opran, A., Amit, Y., Arbel, R., Aro, H., Atar, D., Bishay, M., Borner, M.G., Chiron, P., Choong, P., Cinats, J., Courtenay, B., Feibel, R., Geulette, B., Gravel, C., Haas, N., Raschke, M., Hammacher, E., van der Velde, D., Hardy, P., Holt, M., Josten, C., Ketterl, R.L., Lindeque, B., Lob, G., Mathevon, H., McCoy, G., Marsh, D., Miller, R., Munting, E., Oevre, S., Nordsletten, L., Patel, A., Pohl, A., Rennie, W., Reynders, P., Rommens, P.M., Rondia, J., Rossouw, W.C., Daneel, P.J., Ruff, S., Ruter, A., Santavirta, S., Schildhauer, T.A., Gekle, C., Schnettler, R., Segal, D., Seiler, H., Snowdowne, R.B., Stapert, J., Taglang, G., Verdonk, R., Vogels, L., Weckbach, A., Wentzensen, A., and Wisniewski, T. Recombinant human bone morphogenetic protein-2 for treatment of open tibial fractures: a prospective, controlled, randomized study of four hundred and fifty patients. J Bone Joint Surg Am **84-A,** 2123, 2002.
5. Klimo, P., and Peelle, M.W. Use of polyetheretherketone spacer and recombinant human bone morphogenetic protein-2 in the cervical spine: a radiographic analysis. Spine J **9,** 959, 2009.
6. Chen, N.-F., Smith, Z.A., Stiner, E., Armin, S., Sheikh, H., and Khoo, L.T. Symptomatic ectopic bone formation after off-label use of recombinant human bone morphogenetic protein-2 in transforaminal lumbar interbody fusion. J Neurosurg Spine **12,** 40, 2010.
7. Shah, R.K., Moncayo, V.M., Smitson, R.D., Pierre-Jerome, C., and Terk, M.R. Recombinant human bone morphogenetic protein 2-induced heterotopic ossification of the retroperitoneum, psoas muscle, pelvis and abdominal wall following lumbar spinal fusion. Skeletal Radiol **39,** 501, 2010.
8. Lindley, T.E., Dahdaleh, N.S., Menezes, A.H., and Abode-Iyamah, K.O. Complications associated with recombinant human bone morphogenetic protein use in pediatric craniocervical arthrodesis. J Neurosurg Pediatr **7,** 468, 2011.
9. Anderson, C.L., and Whitaker, M.C. Heterotopic ossification associated with recombinant human bone morphogenetic protein-2 (infuse) in posterolateral lumbar spine fusion: a case report. Spine **37,** E502, 2012.
10. Deutsch, H. High-dose bone morphogenetic protein-induced ectopic abdomen bone growth. Spine J **10,** e1, 2010.
11. Epstein, N.E. Complications due to the use of BMP/INFUSE in spine surgery: the evidence continues to mount. Surg Neurol Int **4,** S343, 2013.
12. Mesfin, A., Buchowski, J.M., Zebala, L.P., Bakhsh, W.R., Aronson, A.B., Fogelson, J.L., Hershman, S., Kim, H.J., Ahmad, A., and Bridwell, K.H. High-dose rhBMP-2 for adults: major and minor complications: a study of 502 spine cases. J Bone Joint Surg Am **95,** 1546, 2013.
13. Shields, L.B., Raque, G.H., Glassman, S.D., Campbell, M., Vitaz, T., Harpring, J., and Shields, C.B. Adverse effects associated with high-dose recombinant human bone morphogenetic protein-2 use in anterior cervical spine fusion. Spine **31,** 542, 2006.
14. Epstein, N.E. Pros, cons, and costs of INFUSE in spinal surgery. Surg Neurol Int **2,** 10, 2011.
15. Perri, B., Cooper, M., Lauryssen, C., and Anand, N. Adverse swelling associated with use of rh-BMP-2 in anterior cervical discectomy and fusion: a case study. Spine J **7,** 235, 2007.
16. Yaremchuk, K.L., Toma, M.S., Somers, M.L., and Peterson, E. Acute airway obstruction in cervical spinal procedures with bone morphogenetic proteins. Laryngoscope **120,** 1954, 2010.
17. Jung, R.E., Fenner, N., Hammerle, C.H., and Zitzmann, N.U. Long-term outcome of implants placed with guided bone regeneration (GBR) using resorbable and non-resorbable membranes after 12–14 years. Clin Oral Implants Res **24,** 1065, 2013.

18. Bottino, M.C., Thomas, V., Schmidt, G., Vohra, Y.K., Chu, T.M., Kowolik, M.J., and Janowski, G.M. Recent advances in the development of GTR/GBR membranes for periodontal regeneration-A materials perspective. Dent Mater **28,** 703, 2012.
19. Cochran, D.L., Schenk, R., Buser, D., Wozney, J.M., and Jones, A.A. Recombinant human bone morphogenetic protein-2 stimulation of bone formation around endosseous dental implants. J Periodontol **70,** 139, 1999.
20. Dimitriou, R., Mataliotakis, G.I., Calori, G.M., and Giannoudis, P.V. The role of barrier membranes for guided bone regeneration and restoration of large bone defects: current experimental and clinical evidence. BMC Med **10,** 81, 2012.
21. Simon, A.M., Manigrasso, M.B., and O'Connor, J.P. Cyclooxygenase 2 function is essential for bone fracture healing. J Bone Miner Res **17,** 963, 2002.
22. Burd, T.A., Hughes, M.S., and Anglen, J.O. Heterotopic ossification prophylaxis with indomethacin increases the risk of long-bone nonunion. J Bone Joint Surg Br **85-B,** 700, 2003.
23. Simon, A.M., and O'Connor, J.P. Dose and time-dependent effects of cyclooxygenase-2 inhibition on fracture-healing. J Bone Joint Surg Am **89,** 500, 2007.
24. Goodman, S., Ma, T., Trindade, M., Ikenoue, T., Matsuura, I., Wong, N., Fox, N., Genovese, M., Regula, D., and Smith, R.L. COX-2 selective NSAID decreases bone ingrowth in vivo. J Orthop Res **20,** 1164, 2002.
25. Giannoudis, P.V., MacDonald, D.A., Matthews, S.J., Smith, R.M., Furlong, A.J., and De Boer, P. Nonunion of the femoral diaphysis. The influence of reaming and non-steroidal anti-inflammatory drugs. J Bone Joint Surg Br **82,** 655, 2000.
26. Martin, G.J., Jr., Boden, S.D., Titus, L., and Einhorn, T.A. Recombinant human bone morphogenetic protein-2 overcomes the inhibitory effect of ketorolac, a nonsteroidal anti-inflammatory drug (NSAID), on posterolateral lumbar intertransverse process spine fusion. Spine **24,** 2188, 1999.
27. Zhang, X., Schwarz, E.M., Young, D.A., Puzas, J.E., Rosier, R.N., and O'Keefe, R.J. Cyclooxygenase-2 regulates mesenchymal cell differentiation into the osteoblast lineage and is critically involved in bone repair. J Clin Invest **109,** 1405, 2002.
28. Harten, R.D., Svach, D.J., Schmeltzer, R., and Uhrich, K.E. Salicylic acid-derived poly(anhydride-esters) inhibit bone resorption and formation in vivo. J Biomed Mater Res A **72,** 354, 2005.
29. Schmeltzer, R.C., Schmalenberg, K.E., and Uhrich, K.E. Synthesis and cytotoxicity of salicylate-based poly(anhydride esters). Biomacromolecules **6,** 359, 2005.
30. Schmeltzer, R.C., Anastasiou, T.J., and Uhrich, K.E. Optimized Synthesis of Salicylate-based Poly(anhydride-esters). Polym Bull (Berl) **49,** 441, 2013.
31. Del Gaudio, C., Bianco, A., and Grigioni, M. Electrospun bioresorbable trileaflet heart valve prosthesis for tissue engineering: in vitro functional assessment of a pulmonary cardiac valve design. Ann Ist Super Sanita **44,** 178, 2008.
32. Heo, S.-J., Nerurkar, N.L., Baker, B.M., Shin, J.-W., Elliott, D.M., and Mauck, R.L. Fiber stretch and reorientation modulates mesenchymal stem cell morphology and fibrous gene expression on oriented nanofibrous microenvironments. Ann Biomed Eng **39,** 2780, 2011.
33. Simonet, M., Schneider, O.D., Neuenschwander, P., and Stark, W.J. Ultraporous 3D polymer meshes by low-temperature electrospinning: use of ice crystals as a removable void template. Polym Eng Sci **47,** 2020, 2007.
34. Schneider, C.A., Rasband, W.S., and Eliceiri, K.W. NIH Image to ImageJ: 25 years of image analysis. Nat Methods **9,** 671, 2012.
35. Smith, P.K., Krohn, R.I., Hermanson, G.T., Mallia, A.K., Gartner, F.H., Provenzano, M.D., Fujimoto, E.K., Goeke, N.M., Olson, B.J., and Klenk, D.C. Measurement of protein using bicinchoninic acid. Anal Biochem **150,** 76, 1985.
36. Oest, M.E., Dupont, K.M., Kong, H.J., Mooney, D.J., and Guldberg, R.E. Quantitative assessment of scaffold and growth factor-mediated repair of critically sized bone defects. J Orthop Res **25,** 941, 2007.
37. Boden, S.D., Zdeblick, T.A., Sandhu, H.S., and Heim, S.E. The use of rhBMP-2 in interbody fusion cages. Definitive evidence of osteoinduction in humans: a preliminary report. Spine **25,** 376, 2000.
38. Cicciu, M., Scott, A., Cicciu, D., Tandon, R., and Maiorana, C. Recombinant human bone morphogenetic protein-2 promote and stabilize hard and soft tissue healing for large mandibular new bone reconstruction defects. J Craniofac Surg **25,** 860, 2014.
39. Friess, W., Uludag, H., Foskett, S., Biron, R., and Sargeant, C. Characterization of absorbable collagen sponges as recombinant human bone morphogenetic protein-2 carriers. Int J Pharm **185,** 51, 1999.
40. Wijdicks, C.A., Virdi, A.S., Sena, K., Sumner, D.R., and Leven, R.M. Ultrasound enhances recombinant human BMP-2 induced ectopic bone formation in a rat model. Ultrasound Med Biol **35,** 1629, 2009.
41. Angle, S.R., Sena, K., Sumner, D.R., Virkus, W.W., and Virdi, A.S. Healing of rat femoral segmental defect with bone morphogenetic protein-2: a dose response study. J Musculoskelet Neuronal Interact **12,** 28, 2012.
42. Maniatopoulos, C., Rodriguez, A., Deporter, D.A., and Melcher, A.H. An improved method for preparing histological sections of metallic implants. Int J Oral Maxillofac Implants **1,** 31, 1986.
43. Amann, R., and Peskar, B.A. Anti-inflammatory effects of aspirin and sodium salicylate. Eur J Pharmacol **447,** 1, 2002.
44. Mitchell, J.A., Saunders, M., Barnes, P.J., Newton, R., and Belvisi, M.G. Sodium salicylate inhibits cyclo-oxygenase-2 activity independently of transcription factor (nuclear factor kappaB) activation: role of arachidonic acid. Mol Pharmacol **51,** 907, 1997.
45. Lansdown, A.B., and Grasso, P. Histological changes in the skeletal system of the developing quail embryo treated with sodium salicylate. Experientia **25,** 885, 1969.
46. Chikazu, D., Li, X., Kawaguchi, H., Sakuma, Y., Voznesensky, O.S., Adams, D.J., Xu, M., Hoshi, K., Katavic, V., Herschman, H.R., Raisz, L.G., and Pilbeam, C.C. Bone morphogenetic protein 2 induces cyclo-oxygenase 2 in osteoblasts via a Cbfa1 binding site: role in effects of bone morphogenetic protein 2 in vitro and in vivo. J Bone Miner Res **17,** 1430, 2002.
47. Arikawa, T., Omura, K., and Morita, I. Regulation of bone morphogenetic protein-2 expression by endogenous prostaglandin E2 in human mesenchymal stem cells. J Cell Physiol **200,** 400, 2004.
48. Susperregui, A.R., Gamell, C., Rodriguez-Carballo, E., Ortuno, M.J., Bartrons, R., Rosa, J.L., and Ventura, F. Noncanonical BMP signaling regulates cyclooxygenase-2 transcription. Mol Endocrinol **25,** 1006, 2011.
49. Mitchell, A., Kim, B., Cottrell, J., Snyder, S., Witek, L., Ricci, J., Uhrich, K.E., and O'Connor, J.P. Development of

a guided bone regeneration device using salicylic acid-poly(anhydride-ester) polymers and osteoconductive scaffolds. J Biomed Mater Res A **102A,** 655, 2013.
50. Lapenna, D., Ciofani, G., Pierdomenico, S.D., Neri, M., Cuccurullo, C., Giamberardino, M.A., and Cuccurullo, F. Inhibitory activity of salicylic acid on lipoxygenase-dependent lipid peroxidation. Biochim Biophys Acta **1790,** 25, 2009.
51. Cottrell, J.A., and O'Connor, J.P. Pharmacological inhibition of 5-lipoxygenase accelerates and enhances fracture-healing. J Bone Joint Surg Am **91,** 2653, 2009.
52. Manigrasso, M.B., and O'Connor, J.P. Accelerated fracture healing in mice lacking the 5-lipoxygenase gene. Acta Orthop **81,** 748, 2010.
53. Cronstein, B.N., Van de Stouwe, M., Druska, L., Levin, R.I., and Weissmann, G. Nonsteroidal antiinflammatory agents inhibit stimulated neutrophil adhesion to endothelium: adenosine dependent and independent mechanisms. Inflammation **18,** 323, 1994.
54. Cronstein, B.N., Montesinos, M.C., and Weissmann, G. Salicylates and sulfasalazine, but not glucocorticoids, inhibit leukocyte accumulation by an adenosine-dependent mechanism that is independent of inhibition of prostaglandin synthesis and p105 of NFkappaB. Proc Natl Acad Sci U S A **96,** 6377, 1999.
55. Carroll, S.H., Wigner, N.A., Kulkarni, N., Johnston-Cox, H., Gerstenfeld, L.C., and Ravid, K. A2B adenosine receptor promotes mesenchymal stem cell differentiation to osteoblasts and bone formation in vivo. J Biol Chem **287,** 15718, 2012.
56. Mediero, A., and Cronstein, B.N. Adenosine and bone metabolism. Trends Endocrinol Metab **24,** 290, 2013.
57. Carbone, A.L., and Uhrich, K.E. Design and synthesis of fast-degrading poly(anhydride-esters). Macromol Rapid Commun **30,** 1021, 2009.
58. Schmeltzer, R.C., and Uhrich, K.E. Synthesis and characterization of salicylic acid-based poly(anhydride-ester) copolymers. J Bioact Compat Polym **21,** 123, 2006.
59. Prudencio, A., Schmeltzer, R.C., and Uhrich, K.E. Effect of linker structure on salicylic acid-derived poly(anhydride-esters). Macromolecules **38,** 6895, 2005.
60. Whitaker-Brothers, K., and Uhrich, K. Poly(anhydride-ester) fibers: role of copolymer composition on hydrolytic degradation and mechanical properties. J Biomed Mater Res A **70,** 309, 2004.
61. Sun, H., Mei, L., Song, C., Cui, X., and Wang, P. The in vivo degradation, absorption and excretion of PCL-based implant. Biomaterials **27,** 1735, 2006.
62. Lam, C.X., Hutmacher, D.W., Schantz, J.T., Woodruff, M.A., and Teoh, S.H. Evaluation of polycaprolactone scaffold degradation for 6 months in vitro and in vivo. J Biomed Mater Res A **90,** 906, 2009.

Address correspondence to:
J. Patrick O'Connor, PhD
Department of Microbiology, Biochemistry and Molecular Genetics
New Jersey Medical School
Rutgers, The State University of New Jersey
185 South Orange Avenue
Newark, NJ 07013

E-mail: oconnojp@njms.rutgers.edu

Received: July 30, 2014
Accepted: March 16, 2015
Online Publication Date: April 29, 2015